

## Article

# Comparative Studies of Piston Crown Coating with YSZ and $\text{Al}_2\text{O}_3\cdot\text{SiO}_2$ on Engine out Responses Using Conventional Diesel and Palm Oil Biodiesel

Navin Ramasamy<sup>1</sup>, Mohammad Abul Kalam<sup>1,\*</sup>, Mahendra Varman<sup>1</sup> and Yew Heng Teoh<sup>2,\*</sup>

<sup>1</sup> Center for Energy Science, Faculty of Engineering, Universiti Malaya, Kuala Lumpur 50603, Malaysia; navin.ramasamy@yahoo.com (N.R.); mahendra@um.edu.my (M.V.)

<sup>2</sup> School of Mechanical Engineering, Universiti Sains Malaysia, Nibong Tebal 14300, Malaysia

\* Correspondence: kalam@um.edu.my (M.A.K.); yewhengteoh@usm.my (Y.H.T.)

**Abstract:** In this study, the effect of a thermal barrier coating with yttria-stabilized zirconia (YSZ) and aluminum silicate ( $\text{Al}_2\text{O}_3\cdot\text{SiO}_2$ ) alongside an NiCrAl bond coat on the engine performance and emission analysis was evaluated by using conventional diesel and pure palm oil biodiesel. These materials were coated on the piston alloy via plasma spray coating. The findings demonstrated that YSZ coating presented better engine performances, in terms of brake thermal efficiency (BTE) and brake-specific fuel consumption (BSFC) for both fuels. The piston with YSZ coating materials achieved the highest BTE (15.94% for diesel, 14.55% for biodiesel) and lowest BSFC (498.96 g/kWh for diesel, 619.81 g/kWh for biodiesel). However,  $\text{Al}_2\text{O}_3\cdot\text{SiO}_2$  coatings indicated better emission with lowest emissions of NO, CO, and  $\text{CO}_2$  for both diesel and biodiesel. For the uncoated piston, the results indicated that the engine clocked the highest torque and power, especially on diesel fuel due to the high viscosity and low caloric value, and it recorded the lowest hydrocarbon emission due to the complete combustion of fuel in the engine. Hence, it was concluded that the YSZ coating could lead to better engine performance, while  $\text{Al}_2\text{O}_3\cdot\text{SiO}_2$  showed promising results in terms of greenhouse gas emission.

**Keywords:** thermal barrier coating; palm oil biodiesel; diesel engine



**Citation:** Ramasamy, N.; Abul Kalam, M.; Varman, M.; Teoh, Y.H. Comparative Studies of Piston Crown Coating with YSZ and  $\text{Al}_2\text{O}_3\cdot\text{SiO}_2$  on Engine out Responses Using Conventional Diesel and Palm Oil Biodiesel. *Coatings* **2021**, *11*, 885. <https://doi.org/10.3390/coatings11080885>

Academic Editor: Csaba Balázs

Received: 23 June 2021

Accepted: 15 July 2021

Published: 23 July 2021

**Publisher's Note:** MDPI stays neutral with regard to jurisdictional claims in published maps and institutional affiliations.



**Copyright:** © 2021 by the authors. Licensee MDPI, Basel, Switzerland. This article is an open access article distributed under the terms and conditions of the Creative Commons Attribution (CC BY) license (<https://creativecommons.org/licenses/by/4.0/>).

## 1. Introduction

There has been continuous improvement in the combustion chemistry and desired product of combustion over the years. For instance, the discovery of alternative liquid fuels as one of the optimum solutions to improve combustion. The geometrical or mechanical aspect of the combustion chamber should be critically considered in order to achieve better performance and less emissions. Malaysia is generally one of the world's main producers of palm oil. Palm oil has been identified as one of the reliable sources of alternative fuels in Malaysia. Numerous matured palm oil biodiesel factories in Malaysia have been operating successfully and have managed to sell their products to local and global users [1,2]. The use of palm biodiesel in the compression ignition (CI) engine typically reduces brake thermal efficiency (BTE), unburned hydrocarbon, and carbon monoxide and increases brake-specific fuel consumption (BSFC) and nitrogen oxide [3]. In the CI engine, the use of a piston bowl significantly influences the mixing of fuel and air. In the case of a direct injection CI engine, the use of a piston of the deep troidal bowl type provides a better and faster swirl of air intake with a proper mixture ratio, better firing, and complete burns and improves the torque value by 3–5%. Based on simulation results, the troidal bowl piston has been found to reduce the BSFC of the engine [4].

The thermal barrier coating (TBC) is a common term in the industry that describes the coating advantages of improved thermal efficiency. Coating technologies have their own ways to enhance green technologies with proven results of improvement in BSFC

and lower emissions and smoke opacity [5]. The thermal barrier coating of a piston crown is commonly made of ceramic material, but most studies have focused on the stabilized zirconia with various compositions, such as zirconia oxide ( $ZrO_2$ ), partially stabilized zirconium (PSZ), yttria-stabilized zirconia (YSZ) [5], magnesia-stabilized zirconia (MSZ) [6], and PEO ( $Al_2O_3 \cdot ZrO_2 \cdot SiO_2$ ) [7,8]. YSZ is considered as a good choice for thermal barrier coatings as this coating material offers several advantages, such as a high thermal expansion coefficient, low thermal conductivity, and high thermal shock resistance [9]. YSZ is commonly used in the industry to coat blades in gas turbine engines in order to achieve better thermal efficiency [10,11]. Some of these ceramic coatings for diesel engines were tested using Pongamia oil [12], cotton seed oil [13], crude Jatropha oil with carbureted oil [14], and diesel fuel [15], which revealed significantly improved thermal efficiency. Nanoscale or topographic characterization of three-dimensional surfaces enables modeling of the surface behavior of the coated piston [16]. It has been determined that fractal analysis is important in understanding the growth of structures during different manufacturing processes and developing fractal-like structures for enhanced performance in coating applications [17].

The present study focused on the research gaps found in the literature on alternative fuels in the automotive field, with the aim to improve, enhance, or eliminate these gaps using an engineered mechanical solution, specifically through the adoption of coating technologies enhancement in the diesel engine. There are several disadvantages of biodiesel, such as higher viscosity and low calorific value—in this case, more fuel for burning is required in order to achieve the same performance as the other conventional fuels [18]. Furthermore, the oxygen content in vegetable oils increases the exhaust  $NO_x$  level [19]. Generally, the application of biodiesel as fuel offers several advantages, such as being a renewable resource, having a high cetane number, possessing lower content of sulphur and aromatic compounds, and emitting lower content of carbon monoxide (CO), unburned hydrocarbons, and particulate matters [20]. The  $NO$  values in relation to the thermal barrier coating were found to be higher than those of uncoated piston, which indicated the need for research to address this gap. The  $NO$  value typically increases with the increase of heat. Hence, for this experimental work, only the piston crown was coated and the  $NO$  value was expected to be reduced since heat was partially contained. Meanwhile, the combination of triphase composite ceramic coating,  $Al_2O_3 \cdot ZrO_2$ , and a small amount of  $SiO_2$  (SiASZ) presents good thermal shock resistance [8]. However, the  $Al_2O_3 \cdot SiO_2$  coating for the engine was never tested and the outcomes of Kubota RT125 engine (Kubota, Osaka, Japan) performance and emission analysis were never evaluated for B100 palm oil biodiesel. This particular coating material was expected to further improve the emissions, as it possesses high thermal insulation capability and its combination with  $SiO_2$  potentially improves the  $NO$  emission. This experimental work aimed to evaluate the effect of a piston crown coating with YSZ and  $Al_2O_3 \cdot SiO_2$  on the engine performance and exhaust emissions.

## 2. Materials and Methods

Figure 1 shows the schematic view of the experimental test setup, which included a single-cylinder, four stroke, direct injection diesel engine. The details of the test engine (Kubota RT 125, Kubota, Osaka, Japan) are presented in Table 1. Figure 2 indicates the experimental setup, which included an eddy current dynamometer to alter or tune the engine load. For this experimental test setup, a generator-type dynamometer was included to hold the engine load and speed. The function of the eddy current dynamometer is to provide brake power [21]. Besides that, this experimental test setup was also equipped with a data acquisition system to collect data and analyze the performance of the tested fuels according to various types of piston coatings. The injection system used for this experiment was a direct injection combustion system (KUBOTA RT125DI-ES, Kubota, Osaka, Japan) and the details are shown in Table 1. Besides, the coating on the piston was a 400  $\mu m$  thick thermal barrier coating with an 100  $\mu m$  lining layer of NiCrAl [13].

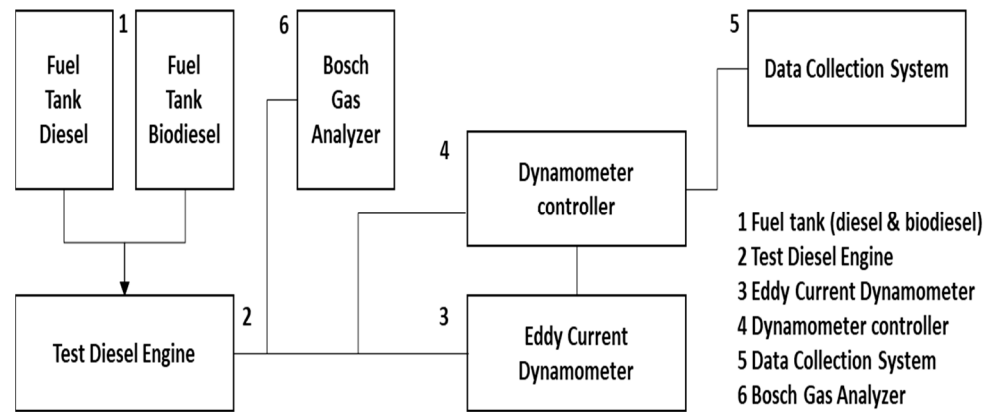


Figure 1. Schematic diagram for the experimental setup.

Table 1. Engine Specification.

Model	RT125DI-ES
Type	Water cooled 4 stroke horizontal diesel engine
Cylinder No	1
Bore x Stroke	94 mm × 96 mm
Displacement	666 cc
Max Output	9.2 kW/2400 rpm
Compression Ratio	18:1
Max. Torque	4.7 kgf-m/1600 rpm
Combustion System	Direct injection
Piston Material	High Strength Aluminum Alloy JIS AC8A



Figure 2. Kubota RT-125 diesel engine experimental setup.

For the loading of the engine, an electric dynamometer (KAMA, Fuzhou, China), which can operate at 26 kW, 80 Nm torque, and max 5000 rpm ( $\pm 50$ ), was used. The data obtained during the engine tests were recorded to the computer by the interface of the engine test device depending on the time. Simultaneously with these measurements, emission values were measured from the emission device (BOSCH, Gerlingen, Germany) and recorded by printing them out.

The experimental test was conducted at a temperature of 32 °C and humidity of 61%, according to different speed settings under a fully loaded engine operation condition. According to the manufacturer, the full load engine speed can be achieved at the lowest engine speed of 1000 rpm. However, for safety reasons, the lowest engine test speed in this experimental test was reduced to 1200 rpm since the engine vibration was excessively high during the full load condition. Besides that, the fuel throttle of the engine was set at the maximum condition. Following that, the engine speed was gradually reduced at intervals of 200 rpm from 2400 rpm to 1200 rpm. Expectedly, the dynamometer increased the load applied to the engine in order to achieve the desired speed as the speed decreased. A similar step was repeated for each coated piston and fuel type. Furthermore, each experimental test was repeated three times to obtain the average value. With that, the consistency of the recorded values was ensured with minimal measurement errors. The recorded data were transformed into graph format to facilitate the analysis and observation. Prior to taking each reading, the engine was operated at a steady condition for 5–7 minutes for all tested pistons and fuel types. Data of fuel consumption, torque, power, hydrocarbon, carbon dioxide, oxygen, nitrogen oxide, and carbon monoxide were recorded. All testing and data collection processes were performed using the controller and recorded on the computer. The exhaust emission test was conducted using the BOSCH model emission analyzer (BOSCH, Gerlingen, Germany). This device is equipped with a NO sensor and can measure the smoke opacity with the use of additional probe that is linked to the opacimeter unit. Meanwhile, gravimetric type fuel consumption meter (Kobold, Nordring, Germany) was used to measure fuel flow rate.

This experimental test involved three types of pistons, which included an uncoated piston, YSZ-coated piston crown, and  $\text{Al}_2\text{O}_3\cdot\text{SiO}_2$ -coated piston crown. The thermal barrier coating was built on the piston crown using the plasma spray technique. A small amount of  $\text{SiO}_2$  was introduced and blended into the  $\text{Al}_2\text{O}_3$  coating. NiCrAl was used to bond the thermal barrier coating with the surface of piston crown. Figure 3 presents a schematic diagram for the thermal barrier coating, whereas Figure 4 shows the thermal barrier coating of YSZ and  $\text{Al}_2\text{O}_3\cdot\text{SiO}_2$  on the piston crown.

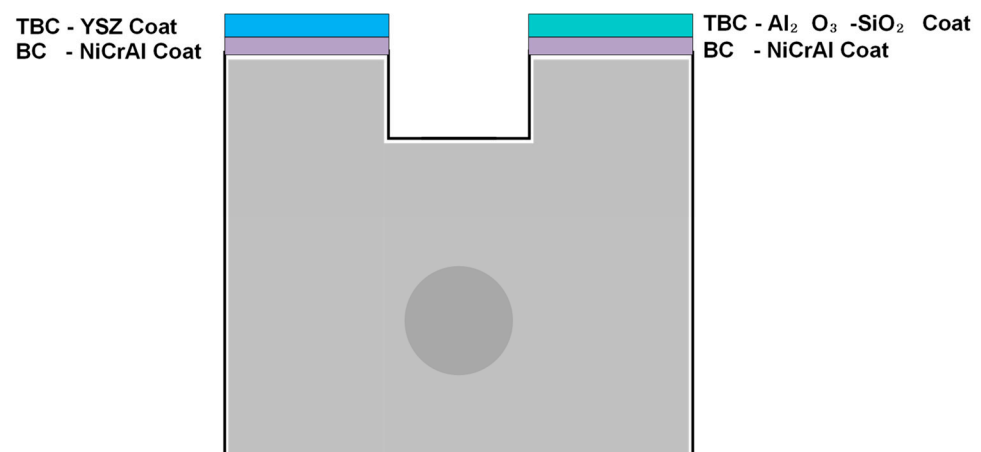


Figure 3. Thermal barrier coating layer on a piston.



**Figure 4.** Piston coated with (a) YSZ and (b)  $\text{Al}_2\text{O}_3\cdot\text{SiO}_2$ .

Both the YSZ and  $\text{Al}_2\text{O}_3\cdot\text{SiO}_2$  were in powder form. By applying plasma spray, the abrasive powder was melted in ionized gas on the piston surface, resulting in the formation of a coating layer on the piston crown. The plasma spray was equipped with a powder feeder, gas supply, spray gun, power unit, controller, cooling unit, and holder. The ceramic coating materials of YSZ (purity 99.9%) and  $\text{Al}_2\text{O}_3\cdot\text{SiO}_2$  (purity 99.9%) used in this experimental test were readily available. Prior to the application of coating, acetone was used to clean the surface of the piston and the process proceeded with grit blasting to increase its surface roughness in order to enhance the grip of the coating to the surface of the piston.

$\text{Al}_2\text{O}_3\cdot\text{SiO}_2$  is a fused and crushed material developed specifically for application using plasma spray as part of a TBC. The SEM of  $\text{Al}_2\text{O}_3\cdot\text{SiO}_2$  powder morphology and microstructure are shown in Figures 5 and 6, respectively. The typical material characteristic of  $\text{Al}_2\text{O}_3\cdot\text{SiO}_2$  is presented in Table 2.  $\text{Al}_2\text{O}_3\cdot\text{SiO}_2$  has lower thermal expansion compared to YSZ. Furthermore,  $\text{Al}_2\text{O}_3\cdot\text{SiO}_2$  also delivers low thermal conductivity, is superior in abrasion resistance, and has higher phase stabilization through the life span of the coating, with an allowable operating temperature in combustion engine operations.

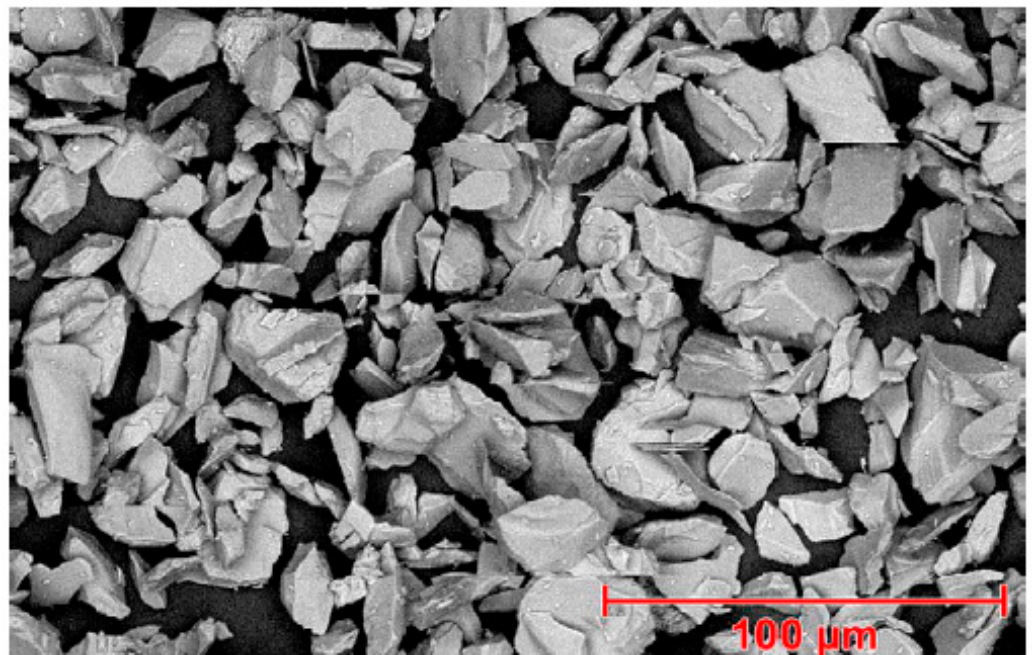


**Figure 5.** SEM photomicrographs ( $1000\times$  of magnification) of  $\text{Al}_2\text{O}_3\cdot\text{SiO}_2$  powder morphology [22].

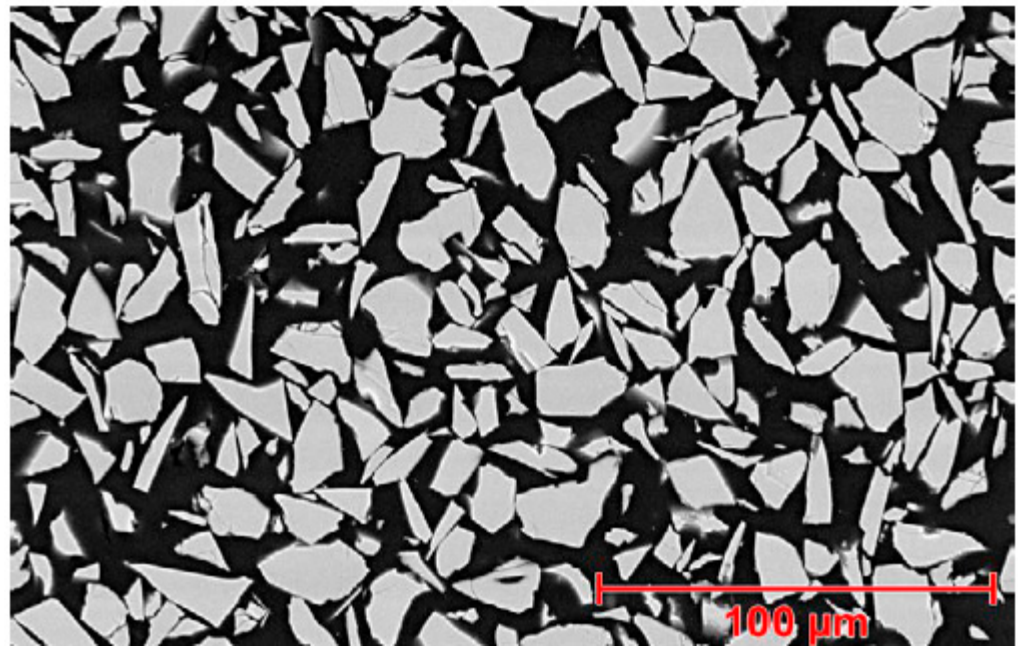


Figure 6. SEM photomicrographs of  $\text{Al}_2\text{O}_3\cdot\text{SiO}_2$  microstructure [22].

Table 2.  $\text{Al}_2\text{O}_3\cdot\text{SiO}_2$  Material (Oerlikon Metco, Shanghai, China) Characteristics.

Classification		Ceramic, Aluminum Silicate	
Chemistry		$3\text{Al}_2\text{O}_3\cdot 2\text{SiO}_2$	
Manufacture		Fused & Crushed	
Morphology		Irregular	
Thermal Expansion Coefficient		$5\text{--}6 \times 10^{-6}/^\circ\text{C}$	
Thermal Conductivity		2.5–3.5 W/mK	
Service Temperature		$\leq 1300^\circ\text{C}$	
Chemical Composition	Weight percentage (nominal)	$\text{Al}_2\text{O}_3$	Balance
		$\text{SiO}_2$	23–28
		Other Oxides	1 max
Powder Characteristics	Nominal range ( $\mu\text{m}$ )		–45 + 5
	D90		35–40
	D50		20–25
	D10		10–15

The YSZ was fused, pre-alloyed and crushed into a powder form with consistent sizing before being sprayed dry. The spheroidal shape, as per Figure 7, promotes chemical homogeneousness, structural stability, and exceptional flow that enhances life span and reliability of TBC. The typical material characteristic of YSZ is presented in Table 3 and TBC working parameters are presented in Table 4. Powders formed with fine particle distributions, such as YSZ compared to  $\text{Al}_2\text{O}_3\cdot\text{SiO}_2$ , archetypally produce dense coating microstructures that show better material deposit characteristics for TBC.

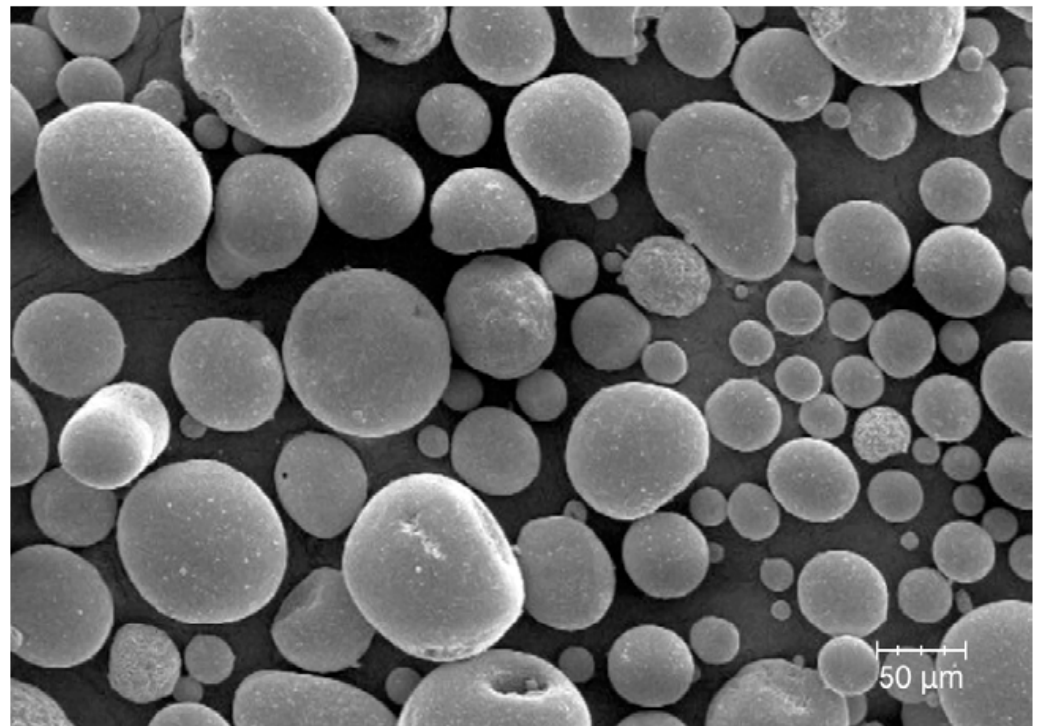


Figure 7. SEM photomicrographs (1000 × of magnification) of YSZ powder morphology [23].

Table 3. YSZ Material (Oerlikon Metco, Shanghai, China) Characteristics.

<b>Classification</b>	Ceramic, Zirconia Based	
<b>Chemistry</b>	$ZrO_2 \cdot 8Y_2O_3$	
<b>Manufacture</b>	Agglomerated & HOSP™	
<b>Morphology</b>	Spheroidal	
<b>Thermal Expansion Coefficient</b>	$10 \times 10^{-6} / ^\circ C$	
<b>Thermal Conductivity</b>	0.8–1.3 W/mK	
<b>Service Temperature</b>	$\leq 1250 \text{ } ^\circ C$	
<b>Chemical Composition</b>	ZrO <sub>2</sub>	Balance
	Y <sub>2</sub> O <sub>3</sub>	7.0–9.0
	SiO <sub>2</sub>	0.7
	TiO <sub>2</sub>	0.2
	Al <sub>2</sub> O <sub>3</sub>	0.2
	Fe <sub>2</sub> O <sub>3</sub>	0.2
	Monoclinic Phase	~6
<b>Powder Characteristics</b>	Nominal range (μm)	−125 + 11
	D90	93–103
	D50	50–57
	D10	21–25

Table 4. TBC Working Parameters.

Parameter	YSZ	Al <sub>2</sub> O <sub>3</sub> ·SiO <sub>2</sub>
Voltage	20 kV	20 kV
Working distance	15 mm	15 mm
Rotating Speed	25 rpm	25 rpm
Temperature	$800 \pm 50 \text{ } ^\circ C$	$800 \pm 50 \text{ } ^\circ C$

In addition, the tested fuels were the commercial diesel and B100 palm biodiesel. Table 5 lists the thermal barrier coatings used in this study, while Table 6 lists the physical and chemical properties of the biodiesel and diesel fuels.

**Table 5.** List of Thermal Barrier Coating Mixtures.

Coating Mixtures	Fuel	Acronyms	Note
Uncoated	Diesel	P1D	Piston Type 1 Diesel
	B100 Palm	P1B	Piston Type 1 Biodiesel
Coated 100% YSZ	Diesel	P2D	Piston Type 2 Diesel
	B100 Palm	P2B	Piston Type 2 Biodiesel
Coated 100% Al <sub>2</sub> O <sub>3</sub> ·SiO <sub>2</sub>	Diesel	P3D	Piston Type 3 Diesel
	B100 Palm	P3B	Piston Type 3 Biodiesel

**Table 6.** List of the Physical and Chemical Properties of the Biodiesel and Diesel fuels.

Properties	Diesel	B100 Palm Biodiesel
Density at 18 °C (g/m <sup>3</sup> )	0.8210	0.8833
Kinematic viscosity at 35 °C (mm <sup>2</sup> /s)	2.5	4.30
Calorific value (kJ/kg)	42,950	38,108
Cetane number	46	52
Flash point (°C)	50	140

### 3. Results

All the equipment was calibrated by a local specialist (BOSCH, Germany). The engine condition with wide open throttle with varied speed conditions produced the results given in this study. The inaccuracies connected to the equipment's "accuracy level" for measured data were, nevertheless, reduced. The experimental test was repeated three times, and the variation in test results was calculated to determine the amount of uncertainty. In the Table 7, there is a sample calculation. The level of uncertainty was less than 6%, and the error bar was well-fit for presentation in all graphs.

**Table 7.** Uncertainty calculation for HC emission of palm biodiesel engines for coated 100% Al<sub>2</sub>O<sub>3</sub>·SiO<sub>2</sub>.

Three Tests			Max–Min Value		Analyzer Accuracy		Average	% Uncertainty *	
Test 1	Test 2	Test 3	Max	Min	+1 ppm	−1 ppm	ppm	+	−
ppm	ppm	ppm	ppm	ppm					
83	83	79	83	79	84	78	81	3.70	−3.70
54	53	52	54	52	55	51	53	3.77	−3.77
28	27	28	28	27	29	26	27.5	5.45	−5.45
27	26	27	27	26	28	25	26.5	5.66	−5.66
21	21	22	22	21	23	20	21.5	6.98	−6.98
20	20	20	20	20	21	19	20	5.00	−5.00
23	22	23	23	22	24	21	22.5	6.67	−6.67
								5.32	(5.32)

\* Uncertainty value of HC emission for palm biodiesel engines for coated 100% Al<sub>2</sub>O<sub>3</sub>·SiO<sub>2</sub> ± 5.32.

#### 3.1. Exhaust Emission Analysis

Figure 8 presents the trend of hydrocarbon emissions at the variable speed for coated and uncoated pistons. The results indicated that YSZ (P2D and P2B) yielded the lowest hydrocarbon emissions, followed by Al<sub>2</sub>O<sub>3</sub>·SiO<sub>2</sub> (P3D and P3B) and, lastly, uncoated piston (P1D and P1B). These results were found to be similar to the reported results of several prior studies [24–26]. Basically, the combustion chamber and piston head in a standard engine

generated lesser heat compared to the use of coated piston; thus, it affects the evaporation capability of the tested fuels. The YSZ-coated engine recorded a better fuel evaporation rate due to the increased temperature in the combustion chamber and coated piston crown. The higher combustion temperature due to the thermal barrier coating makes fuel burning easier and effective [27]. Besides that, the thermal barrier coating initiated a faster rate of breaking hydrocarbon into hydrogen and oxygen, then mixed with an excess of oxygen available in the combustion chamber, therefore lower hydrocarbon emissions were recorded for coated piston [24]. Other factors, such as quenching distance or flammability limit, also should be included when discussing reduction of hydrocarbon emissions when applying a thermal barrier coating [28]. In addition, B100 palm biodiesel was found to yield lower hydrocarbon emissions compared to the conventional diesel. At the maximum load of 1200 rpm, P1D recorded the lowest hydrocarbon emission (61 ppm), followed by P3D (86 ppm) and P2D (97 ppm). As for the engine operation with biodiesel, P1B recorded the lowest hydrocarbon emission (41 ppm), followed by P3B (82 ppm), and P2B (92 ppm). Biodiesel enhances oxygen content, resulting in better combustion and, subsequently, lower hydrocarbon emissions [29,30]. The obtained results also revealed that P3D and P3B yielded lower hydrocarbon content, followed by P1D, P2B, P1B, and P2D, at the maximum speed of 2400 rpm. Referring to the decreasing trend of hydrocarbon emissions with increasing speed in Figure 8, the study proved that the increase of speed does affect the hydrocarbon emissions.

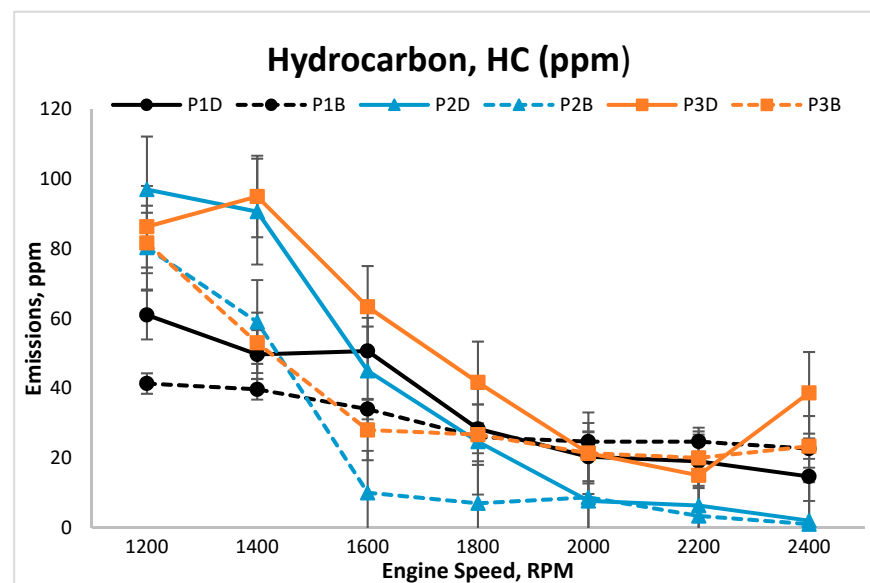


Figure 8. Hydrocarbon emissions at the variable engine speeds.

The oxidation chemistry was found to be suppressed due to the limited availability of oxygen in the air–fuel mixture at the lower speed; at the higher speed, the coated engine, particularly the YSZ-coated engine, was found to perform well for both tested fuels. Overall, the experimental results revealed that the use of biodiesel yielded lower hydrocarbon emissions compared to the use of diesel. Besides that, P2D and P2B were found to maintain good stability and release the lowest hydrocarbon emissions for both tested fuels across all engine speed settings. Unlike the uncoated piston, the  $\text{Al}_2\text{O}_3\text{-SiO}_2$ -coated piston demonstrated fair performance due to the presence of metal ions (aluminum) as the base material of the piston.

Figure 9 shows the trend of NO emissions at the variable speeds for coated and uncoated pistons. Unlike the uncoated piston, both YSZ- and  $\text{Al}_2\text{O}_3\text{-SiO}_2$ -coated pistons were found to substantially reduce NO emissions. All pistons, with or without the coating layer, yielded lower NO emissions as the engine speed increased. However, most prior studies reported increased NO emissions due to the use of a thermal barrier coating [9,29]. This

may be due to the case of high flame temperature and the shorter duration of combustion chemistry in the combustion chamber. [25] The addition of a thermal barrier coating increased the interaction of nitrogen and oxygen at high temperatures, resulting in higher emissions of NO. The production of NO involves the reaction between the formed hydroxide (OH) ions and nitrogen atoms. The increase of the duration of combustion and the use of trapezoidal pistons were found to yield better performances in terms of NO emissions. The trapezoidal piston extended the duration of combustion with the swirl effect, which ensured enhanced mixing of air and fuel, resulting in complete combustion. The reduction of flame temperature and enhancement of the complete combustion further reduced the NO emission. In this study, the  $\text{Al}_2\text{O}_3\cdot\text{SiO}_2$ -coated piston recorded excellent reduction of NO, as compared to YSZ-coated piston. As reported in numerous prior studies, YSZ coating was found to contribute higher NO emission compared to uncoated piston [5]. However, the present study found otherwise, where the use of  $\text{Al}_2\text{O}_3\cdot\text{SiO}_2$  coating contributed to lower NO emission, as compared to YSZ coating. On the other hand, at the lowest speed, the load was found to be higher and NO emission was found to be higher for biodiesel, which may be attributed to the increase in the amount of fuel (for burning) in the combustion chamber.

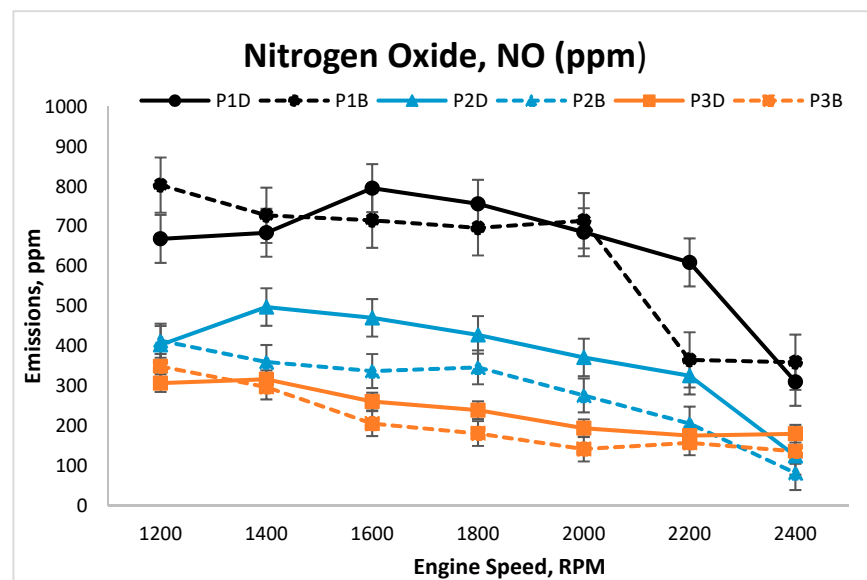
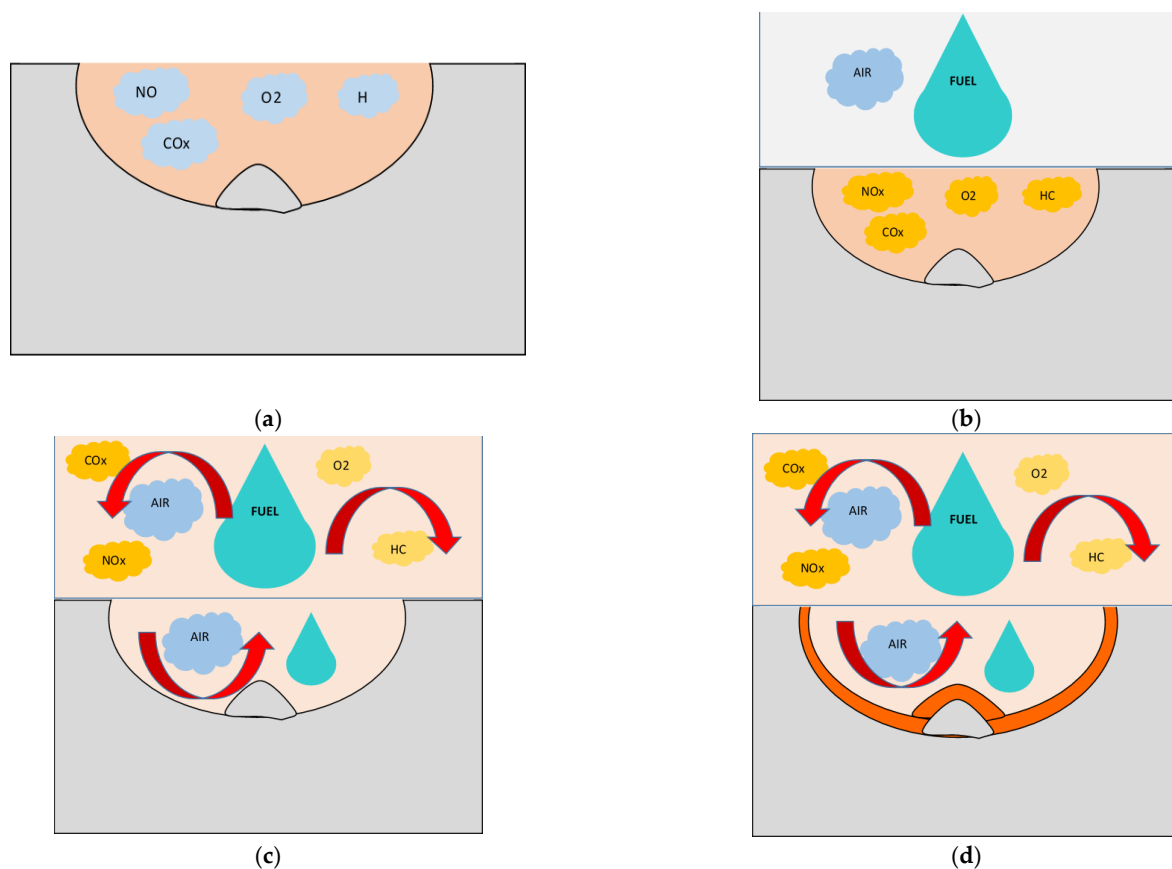


Figure 9. Nitrogen oxide (NO) emission at the variable speed.

For all uncoated and coated pistons in the case of diesel, P3D recorded the lowest NO emission (307 ppm), followed by P2D (403 ppm), and P1D (669 ppm). Meanwhile, as for the case of biodiesel, P3B recorded the lowest NO emission (349 ppm), followed by P2B (414 ppm), and P1B (803 ppm). Overall, the use of biodiesel was found to perform better in reducing NO emissions as compared to the use of diesel. Additionally, P3D and P3B were found to maintain good stability and release the lowest NO emissions for both tested fuels across all engine speed settings. These findings proved that the impact of the thermal barrier coating in reducing NOx emissions, one environmental pollution source that should be controlled [31].

There are three mechanisms that contribute to the production of NOx. The initiation process of thermal NOx is produced through the reaction between nitrogen and oxygen at high temperatures. Higher temperatures in the combustion chamber increase the formation of NOx. Secondly, the rapid reaction of hydrocarbon, nitrogen, and oxygen produces prompt NOx. Prompt NOx is potentially a primary contributor to combustion at low temperatures. Thirdly, fuel NOx is formed along with the excess oxygen combustion of nitrogen-containing organic compounds. The earlier adoption of a sub-stoichiometric combustion process can reduce the formation of NOx [32].

The trapezoidal-shaped piston provides the swirl effect and acts as a staged combustion. A portion of the product of combustion from the immediate previous combustion cycle is temporarily stored in the mixing compartment of the trapezoidal-shaped piston. The products of combustion remain in the heated zone, as illustrated in Figure 10. This staged combustion acts as a preheat agent that introduces the subsequent fuel and air into the combustion chamber. The product of combustion, which mainly contains NO<sub>x</sub>, CO<sub>2</sub>, and HC, enhances the fuel-rich condition. The combination of preheating from staged combustion, improved mixing of combustion products, the swirl effect from the trapezoidal-shaped piston, and the fuel-rich condition helps in the formation of combustion intermediates, resulting in the destructivity of the previously formed NO<sub>x</sub>. In the reducing environment, NO acts as an oxidizer to react with the combustion intermediates and produce N<sub>2</sub>.



**Figure 10.** Staged combustion concept: (a) primary combustion, (b) introduction of subsequent fuel, (c) heated subsequent fuel and blend with previous traces product of combustion, (d) staged combustion of (c).

Figure 11 depicts the trend of CO emission at the variable speeds for coated and uncoated pistons. At lower speeds, the coated pistons emitted higher CO compared to the uncoated piston due to the lack of oxidation, lower temperature, and longer settling time. The production of CO decreased with the increase of speed, whereas the CO emission was suppressed to its minimum when the engine was at its optimum speed. At the maximum load, in the case of diesel, P3D recorded the lowest CO emission (5.03%), followed by P1D (5.82%), and P2D (6.13%). Meanwhile, in the case of biodiesel, P1B recorded the lowest CO emission (4.42%), followed by P3B (5.38%), and P2B (5.84%). Overall, the use of biodiesel was found to emit lower amounts of CO, as compared to the use of diesel.

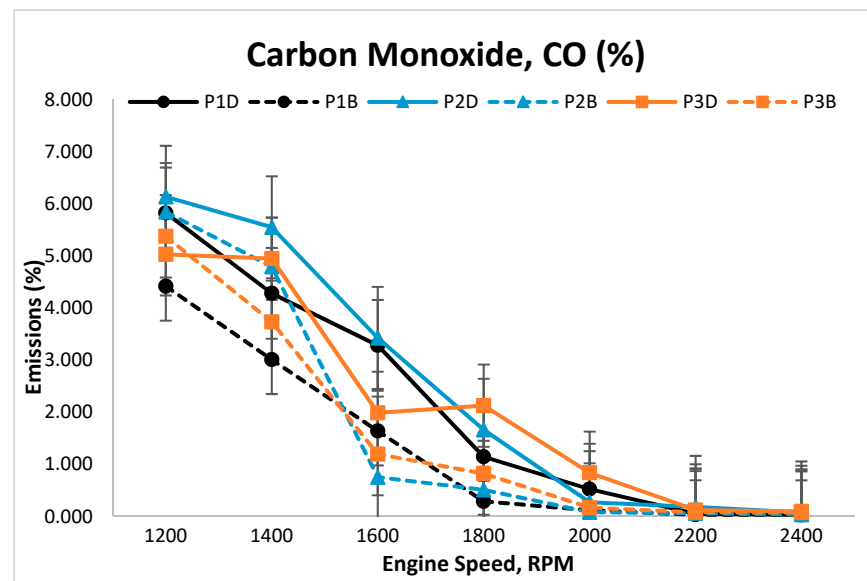


Figure 11. Carbon monoxide (CO) emissions at variable speeds.

The product of incomplete combustion is CO that is commonly found in trace quantities [33]. A low amount of oxygen in the combustion chamber leads to incomplete combustion, which leads to an increase of CO formation. Furthermore, the use of a coated piston has demonstrated higher formation of CO formation, as compared to the use of an uncoated piston, due to the preheat temperature. On the other hand, biodiesel has been found to be the primary supplier of oxygen to the combustion, resulting in lower CO emissions [29]. Besides that, air fuels ratio, compression, combustion cylinder temperature, and amount of oxygen are vital factors for CO formation [34]. Biodiesel containing about 10% of oxygen by mass initiated complete combustion in the chamber, thus reducing CO emissions into the environment [35,36]. The observation also showed the effect of thermal barrier coatings on the CO emissions, with a reduction of CO emissions in coated engines compared to uncoated engines. The thermal insulation of TBC increased the post-compression temperature and then initiated late-phase combustion and oxidation of CO [33]. The pre-heating and mixture of the product of combustion (from the staged combustion) may have contributed to the slight increase of flame temperature.

Figure 12 depicts the trend of CO<sub>2</sub> emissions at the variable speeds for coated and uncoated pistons. At the maximum load, for all coated pistons in the case of diesel, P3D recorded the lowest CO<sub>2</sub> emission (8.10%), followed by P2D (8.52%) and P1D (9.94%). On the other hand, in the case of biodiesel, P3B recorded the lowest CO<sub>2</sub> emission (9.34%), followed by P2B (9.67%) and P1B (10.64%). Overall, the use of biodiesel yielded lower CO<sub>2</sub> emissions compared to the use of diesel. Furthermore, both P3D and P3B were found to maintain good stability and released the lowest CO<sub>2</sub> emissions for both tested fuels. Adding to that, the results also illustrated the effectiveness of the engine in achieving almost complete combustion for both tested fuels. Thus, as shown in Figure 12, the use of diesel contributes to higher CO<sub>2</sub> emission, as compared to the use of biodiesel.

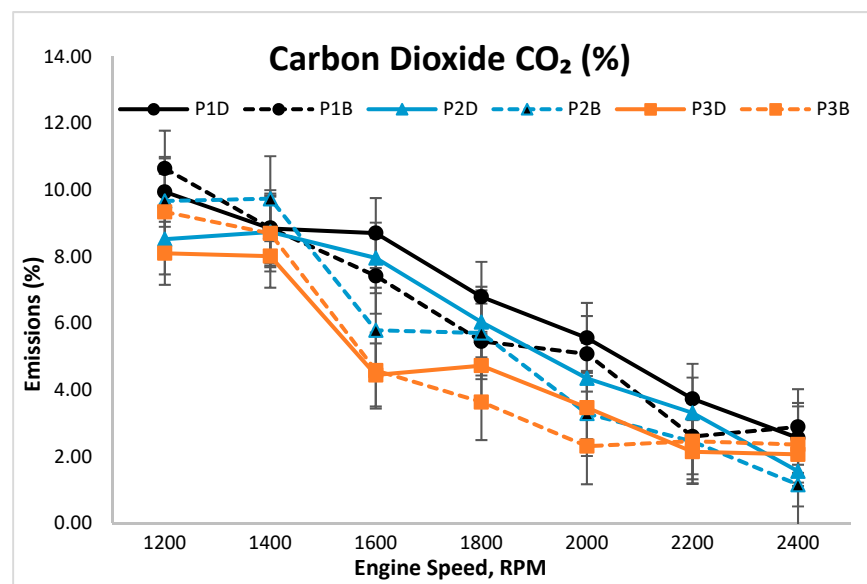


Figure 12. Carbon dioxide (CO<sub>2</sub>) emissions at variable speeds.

### 3.2. Engine Performance

Based on the obtained results in Figure 13, the power and torque developed in the thermal barrier coating engine were reduced for both YSZ-coated and Al<sub>2</sub>O<sub>3</sub>-SiO<sub>2</sub>-coated pistons across all engine speed settings, as compared to the uncoated piston as the baseline. Although the thermal barrier coating insulates the heat and prevents heat reduction for the combustion products, the coating also significantly affects the compression ratio of the engine, which explains the reduction of torque and power in the tested engine [30].

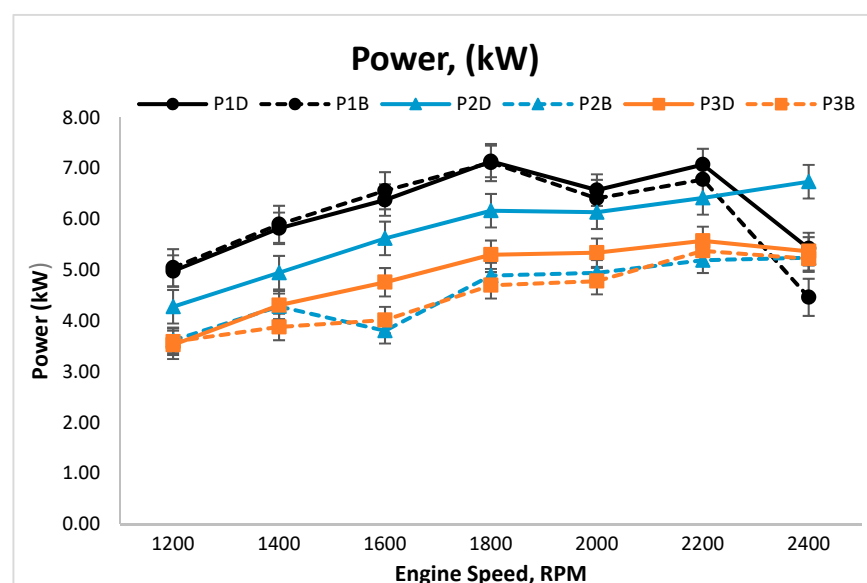


Figure 13. Power (kW) produced at various engine speeds.

At the maximum load, in the case of diesel, P1D recorded the highest power (4.98 kW), followed by P2D (4.28 kW) and P3D (3.53 kW). Meanwhile, in the case of biodiesel, P1B recorded the highest power (5.05 kW), followed by P2B (3.62 kW) and P3B (3.59 kW). Overall, the use of biodiesel was found to produce less power than the use of diesel (as baseline). Similar results were reported in prior studies, where the use of biodiesel generated less power than the use of diesel due to lower heating values and higher kinematic viscosity [34,37]. The results in Figure 14 also revealed the significant impact of coating in

increasing power towards the increase of speed, as at 2400 rpm, P1B recorded the lower power than P2B and P3B. Similar results were also reported in another earlier study, which subsequently reaffirmed this observation [35].

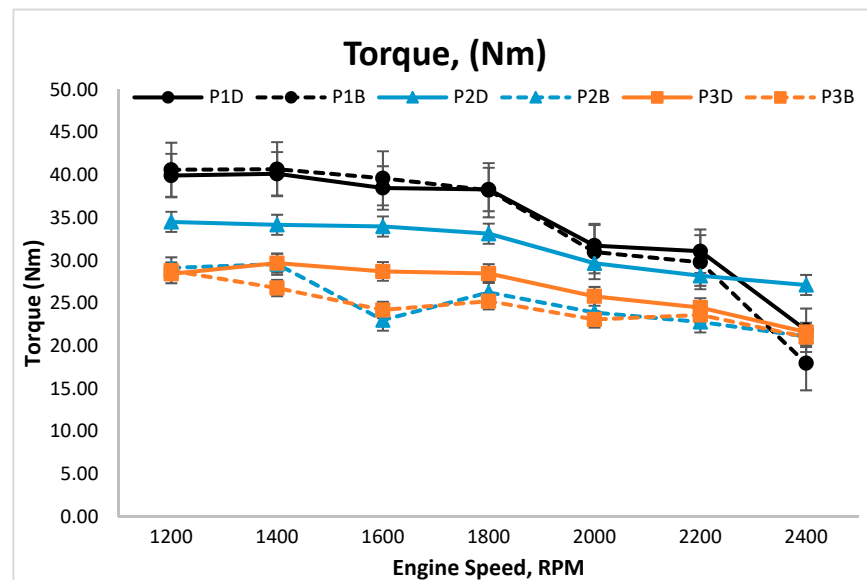


Figure 14. Torque (Nm) produced at variable speeds.

The engine performance is another important criterion when it comes to the internal combustion engine. As presented in Figure 14, the use of biodiesel recorded lower common trends as compared to the use of diesel (as baseline) for both coated and uncoated pistons. Similar results were also reported in several prior studies [37]. This observation can be explained by the combined effect of the relatively higher viscosity and lower caloric value in palm oil biodiesel, as compared to the conventional diesel [38]. At the maximum load, in the case of coated pistons in diesel, P1D recorded the highest torque effect (39.94 Nm), followed by P2D (34.51 Nm) and, lastly, P3D (28.43 Nm). Meanwhile, in the case of biodiesel, P1B recorded the highest torque effect (40.61 Nm), followed by P2B (29.13 Nm) and P3B (28.80 Nm). As for the case of the uncoated piston, the use of biodiesel produced a higher torque effect as compared to the use of diesel. However, for the case of coated pistons, the YSZ-coated piston in biodiesel yielded a lower torque effect than the YSZ-coated piston in diesel, whereas a similar torque effect was produced for  $\text{Al}_2\text{O}_3\cdot\text{SiO}_2$ -coated pistons in both tested fuels. A decrease of torque effect for biodiesel was found in line with the observation of a prior study [38].

BTE and BSFC are other significant factors that determine the performance of an engine. In this study, BSFC was measured within the speed range of 1200 rpm to 2400 rpm for all coated and uncoated pistons under the operational conditions of both diesel and biodiesel. Figure 15 presents the results of BSFC at variable speeds. At the maximum load, in the case of diesel, P2D recorded the lowest BSFC (498.96 g/kWh), followed by P3D (575.16 g/kWh) and, lastly, P1D (609.98 g/kWh). Meanwhile, in the case of biodiesel, P2B recorded the lowest BSFC (619.81 g/kWh), followed by P1B (905.07 g/kWh) and P3B (1229.06 g/kWh). Specifically, in the case of diesel, the results in Figure 15 revealed a slightly higher value of BSFC, with the increase of speed for both YSZ- and  $\text{Al}_2\text{O}_3\cdot\text{SiO}_2$ -coated pistons, as compared to those of uncoated pistons (as baseline). The BSFC values of coated pistons were slightly different from the BSFC values of uncoated pistons. Furthermore, the BSFC for biodiesel was higher than the BSFC for diesel due to lower calorific values of palm oil biodiesel compared to conventional diesel [35]. The load on the engine increases with the decrease in speed. Thus, at the lowest speed of 1200 rpm, where the load was at its highest, both YSZ- and  $\text{Al}_2\text{O}_3\cdot\text{SiO}_2$ -coated pistons reported lower BSFC compared to the BSFC values of uncoated pistons. The temperature in the combustion chamber increased

due to the application of a thermal barrier coating on the piston, which caused the fuel to evaporate easily, resulting in the reduction of BSFC [33]. A low BSFC value indicates that the combustion engine only needs low volume of fuel to produce similar performance to standard engine [27]. In addition, applications of coatings maintain high temperatures in the chamber, preventing heat loss to the surroundings [39].

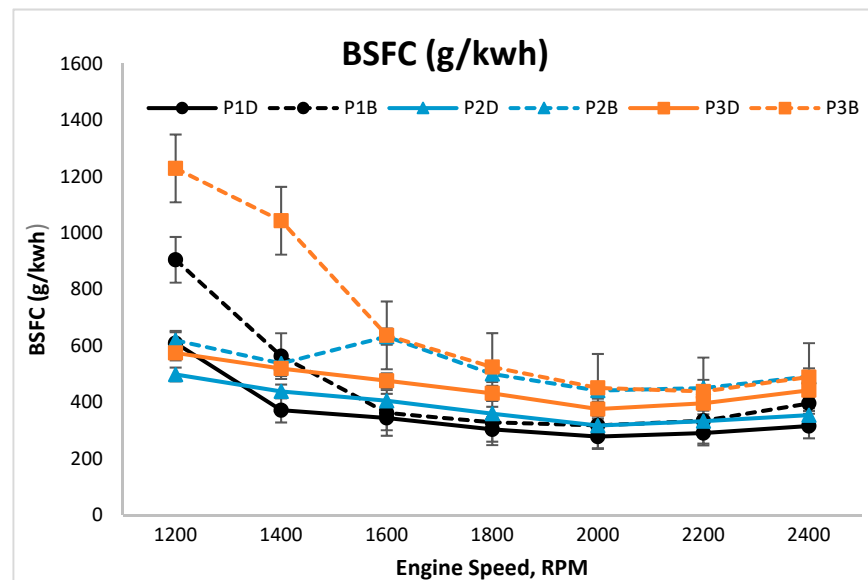


Figure 15. BSFC values at variable speeds.

Figure 16 depicts the trend of BTE at the variable speeds for coated and uncoated pistons. Figure 16 shows a decreasing trend for BTE with the increase of speed for both YSZ- and  $\text{Al}_2\text{O}_3\cdot\text{SiO}_2$ -coated pistons, as compared to the uncoated pistons (as baseline). At the maximum load, in the case of diesel, P2D recorded the highest BTE (15.94%), followed by P3D (13.83%) and P1D (13.04%). Meanwhile, in the case of biodiesel, P2B recorded the highest BTE (14.55%), followed by P1B (9.97%) and P3B (7.34%). Overall, the use of biodiesel recorded lower BTE than the use of diesel, which may be attributed to the poor fuel atomization characteristics, higher flash point, and lower volatility [39–41]. The load on the engine increases when the speed decreases. As compared to the uncoated piston, YSZ- and  $\text{Al}_2\text{O}_3\cdot\text{SiO}_2$ -coated pistons recorded higher BTE. The BTE of uncoated piston reduces with the decrease of engine speed. At lower engine speeds, the output torque is the highest due to the higher amount of fuel injected per cycle, resulting in the generation of higher heat. Hence, YSZ- and  $\text{Al}_2\text{O}_3\cdot\text{SiO}_2$ -coated pistons in this study recorded higher BTE due to the increase of heat for the gas expansion. This may be attributed to better heat insulation and the staged combustion effect of the thermal barrier material that converts more heat into useful works.

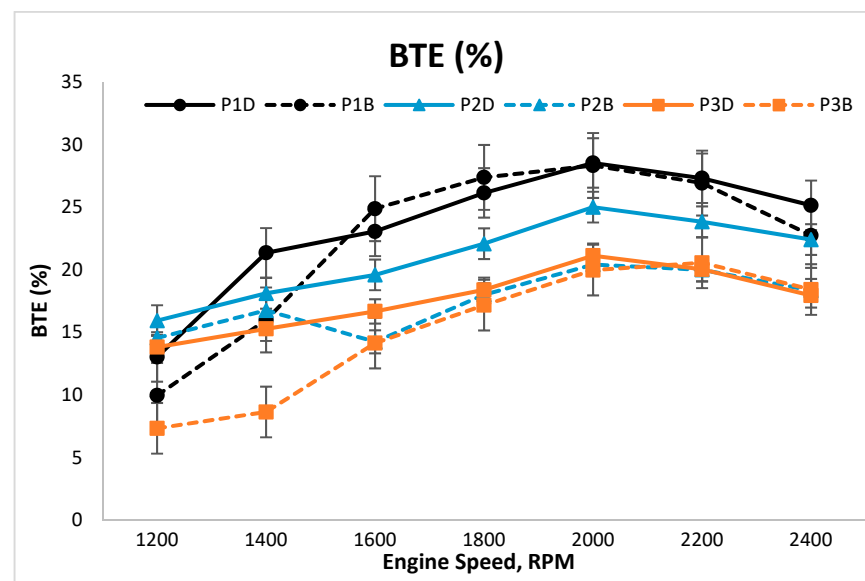


Figure 16. BTE percentage at variable engine speeds.

#### 4. Discussion

This study aimed to evaluate the engine performance and exhaust emissions for an uncoated piston, YSZ-coated piston, and  $\text{Al}_2\text{O}_3\cdot\text{SiO}_2$ -coated piston using conventional diesel and B100 palm biodiesel. In particular, a Kubota RT 125 ES direct engine was used with the eddy current dynamometer. The coating of YSZ and  $\text{Al}_2\text{O}_3\cdot\text{SiO}_2$  was performed using plasma spray coating.  $\text{SiO}_2$  was added to  $\text{Al}_2\text{O}_3$  to enhance the thermal barrier performance. The engine performance and emissions for coated and uncoated pistons for both conventional diesel (as baseline) and B100 palm biodiesel can be concluded as follows:

1. For the case of diesel, the YSZ-coated piston recorded the highest BTE (15.94%). Meanwhile, for the case of biodiesel, the YSZ-coated piston recorded the highest BTE (14.55%). Overall, the use of diesel yielded higher BTE values than the use of biodiesel due to its high calorific value.
2. For the case of diesel, the YSZ-coated piston recorded the lowest BSFC value (498.96 g/kWh). Meanwhile, for the case of biodiesel, the YSZ-coated piston recorded the lowest BSFC value (619.81 g/kWh). Overall, the use of diesel yielded lower BSFC than the use of biodiesel due to the low-density value of diesel.
3. As for the case of diesel, the uncoated piston recorded the highest torque of 39.94 Nm. Meanwhile, as for the case of biodiesel, the uncoated piston recorded the highest torque of 40.61 Nm. Overall, the use of diesel yielded a higher torque effect than the use of biodiesel due to the combined effect of relatively higher viscosity and lower caloric value in palm oil biodiesel compared to diesel.
4. As for the coated pistons under the use of diesel, the uncoated piston recorded the highest power (4.98 kW). Meanwhile, as for the coated pistons under the use of biodiesel, the uncoated piston recorded the highest power (5.05 kW). Overall, the use of diesel yielded higher power than the use of biodiesel, as the thermal barrier coating recorded lower power following the change in the compression ratio.
5. As for the coated pistons under the use of diesel, the  $\text{Al}_2\text{O}_3\cdot\text{SiO}_2$ -coated piston recorded the lowest  $\text{CO}_2$  emission (8.10%). Meanwhile, as for the coated pistons under the use of biodiesel, the  $\text{Al}_2\text{O}_3\cdot\text{SiO}_2$ -coated piston recorded the lowest  $\text{CO}_2$  emission (9.34%).
6. As for the coated pistons under the use of diesel, the  $\text{Al}_2\text{O}_3\cdot\text{SiO}_2$ -coated piston recorded the lowest CO emission (5.03%). Meanwhile, as for the coated pistons under the use of biodiesel, the uncoated piston recorded the lowest CO emission (4.42%).

7. As for the coated pistons under the use of diesel, the  $\text{Al}_2\text{O}_3\cdot\text{SiO}_2$ -coated piston recorded the lowest NO emission (307 ppm). Meanwhile, as for the coated pistons under the use of biodiesel, the  $\text{Al}_2\text{O}_3\cdot\text{SiO}_2$ -coated piston recorded the lowest NO emission (349 ppm). Overall, the use of biodiesel yielded lower NO emissions as compared to the use of diesel. Unlike the uncoated piston, the thermal barrier coating was found to yield a higher temperature for the staged combustion, resulting in the significant reduction of NOx.
8. As for the coated pistons under the use of diesel, the uncoated piston recorded the lowest hydrocarbon emission (61 ppm). Meanwhile, as for the coated pistons under the use of diesel, the uncoated piston recorded the lowest hydrocarbon emission (41 ppm).

## 5. Conclusions

This study produced an overwhelming result in the reduction of emissions, ranging between 50% and 60% of NO emissions using the  $\text{Al}_2\text{O}_3\cdot\text{SiO}_2$  coating compared to uncoated piston. However, the use of the  $\text{Al}_2\text{O}_3\cdot\text{SiO}_2$  coating produced less promising results in regards to the engine performance. Unlike the  $\text{Al}_2\text{O}_3\cdot\text{SiO}_2$ -coated piston, the YSZ-coated piston demonstrated better engine performance. Hence, it is recommended for future research to identify the combination or blend between YSZ and  $\text{Al}_2\text{O}_3\cdot\text{SiO}_2$  in order to balance the gap between both materials.

**Author Contributions:** Conceptualization, N.R., M.A.K., M.V., and Y.H.T.; data curation, N.R.; formal analysis, N.R.; investigation, N.R.; methodology, N.R. and Y.H.T.; resources, M.A.K. and M.V.; supervision, M.A.K. and M.V.; validation, M.A.K., M.V., and Y.H.T.; visualization, N.R.; writing—original draft, N.R.; writing—review and editing, N.R., M.A.K., M.V., and Y.H.T. All authors have read and agreed to the published version of the manuscript.

**Funding:** This research was funded by University of Malaya through the University of Malaya Faculty Research Grant (Grant number: GPF016A-2018), FRGS Research Grant (Grant number: FP142-2019A), and Postgraduate Research Grant (PPP) (Grant number: PG171-2015B).

**Institutional Review Board Statement:** Not applicable.

**Informed Consent Statement:** Not applicable.

**Data Availability Statement:** Data is contained within the article.

**Conflicts of Interest:** The authors declare no conflict of interest.

## References

1. Oguma, M.; Lee, Y.J.; Goto, S. An overview of biodiesel in Asian countries and the harmonization of quality standards. *Int. J. Automot. Technol.* **2011**, *13*, 33–41. [[CrossRef](#)]
2. Johari, A.; Nyakuma, B.B.; Mohd Nor, S.H.; Mat, R.; Hashim, H.; Ahmad, A.; Zakaria, Z.Y.; Tuan Abdullah, T.A. The challenges and prospects of palm oil biodiesel in Malaysia. *Energy* **2015**, *81*, 255–261. [[CrossRef](#)]
3. Gad, M.S.; El-Araby, R.; Abed, K.A.; El-Ibiari, N.N.; El Morsi, A.K.; El-Diwani, G.I. Performance and emissions characteristics of C.I. engine fueled with palm oil/palm oil methyl ester blended with diesel fuel. *Egypt. J. Pet.* **2018**, *27*, 215–219. [[CrossRef](#)]
4. da Silva, M.A.V.; Ferreira, B.L.G.; Marques, L.G.D.C.; Murta, A.L.S.; de Freitas, M.A.V. Comparative study on NOx emissions of biodiesel-diesel blends from soybean, palm and waste frying oils using methyl and ethyl transesterification routes. *Fuel* **2017**, *194*, 144–156. [[CrossRef](#)]
5. Sivakumar, G.; Senthil Kumar, S. Investigation on effect of Ytria Stabilized Zirconia coated piston crown on performance and emission characteristics of a diesel engine. *Alex. Eng. J.* **2014**, *53*, 787–794. [[CrossRef](#)]
6. Cerit, M.; Coban, M. Temperature and thermal stress analyses of a ceramic-coated aluminum alloy piston used in a diesel engine. *Int. J. Therm. Sci.* **2014**, *77*, 11–18. [[CrossRef](#)]
7. Traon, N.; Schnieder, J.; Vilalba, A.; Tonnesen, T.; Telle, R.; Huger, M.; Chotard, T. Influence of Andalusite,  $\text{Al}_2\text{O}_3\text{-ZrO}_2\text{-SiO}_2$  and  $\text{Al}_2\text{O}_3\text{-ZrO}_2$  Addition on Elastic and Mechanical Properties of High Aluminum Castables. *Interceram Int. Ceram. Rev.* **2014**, *63*, 290–294. [[CrossRef](#)]
8. Wang, P.; Li, Y.; Guo, Y.; Wang, J.; Yang, Z.; Liang, M. Effect of zirconia sol on the microstructure and thermal-protective properties of PEO coating on a cast Al-12Si piston alloy. *J. Alloys Compd.* **2016**, *657*, 703–710. [[CrossRef](#)]
9. Krishnamoorthi, T.; Vinayagasundram, G. Performance and emission characteristics analysis of thermal barrier coated diesel engine using palm biodiesel. *Environ. Sci. Pollut. Res.* **2019**, *26*, 11438–11451. [[CrossRef](#)]

10. Clarke, D.R.; Oechner, M.; Padture, N.P. Thermal-barrier coatings for more efficient gas-turbine engines. *MRS Bull.* **2012**, *37*, 891–898. [[CrossRef](#)]
11. Abbas, M.R.; Uday, M.B.; Mohd Noor, A.; Ahmad, N.; Rajoo, S. Microstructural evaluation of a slurry based Ni/YSZ thermal barrier coating for automotive turbocharger turbine application. *Mater. Des.* **2016**, *109*, 47–56. [[CrossRef](#)]
12. Hemanandh, J.; Narayanan, K.V.; Venkatesh, K.; Balaji, K.R.S.; Reddy, L.C.T. Comparative Analysis of Stellite-6 Coated And Uncoated Piston Using Pongamia Biodiesel. *Mater. Today Proc.* **2017**, *5*, 24323–24329. [[CrossRef](#)]
13. Iscan, B. Applications of ceramic coating for improving the usage of cottonseed oil in a diesel engine. *J. Energy Inst.* **2016**, *89*, 150–157. [[CrossRef](#)]
14. Murali Krishna, M.V.S.; Ohm Prakash, T.; Ushasri, P.; Janardhan, N.; Murthy, P.V.K. Experimental investigations on direct injection diesel engine with ceramic coated combustion chamber with carbureted alcohols and crude jatropha oil. *Renew. Sustain. Energy Rev.* **2016**, *53*, 606–628. [[CrossRef](#)]
15. Zhao, H.; Ye, F. Investigation of sputtered WCN coating for diesel engine pistons applications. *Vacuum* **2016**, *126*, 5–6. [[CrossRef](#)]
16. Țălu, Ș. *Micro and Nanoscale Characterization of Three Dimensional Surfaces. Basics and Applications*; Napoca Star Publishing House: Cluj-Napoca, Romania, 2015; pp. 21–27.
17. Mwema, F.M.; Akinlabi, E.T.; Oladijo, O.P.; Fatoba, O.S.; Akinlabi, S.A.; Țălu, Ș. Advances in manufacturing analysis: Fractal theory in modern manufacturing. In *Modern Manufacturing Processes*, 1st ed.; Woodhead Publishing Reviews, Mechanical Engineering Series; Kumar, K., Davim, J.P., Eds.; Woodhead Publishing: Sawston, UK, 2020; Section 1, Chapter 2; pp. 13–19. 246p. [[CrossRef](#)]
18. Dhinesh, B.; Raj, Y.M.A.; Kalaiselvan, C.; KrishnaMoorthy, R. A numerical and experimental assessment of a coated diesel engine powered by high-performance nano biofuel. *Energy Convers. Manag.* **2018**, *171*, 815–824. [[CrossRef](#)]
19. Song, H.; Quinton, K.S.; Peng, Z.; Zhao, H.; Ladommatos, N. Effects of Oxygen Content of Fuels on Combustion and Emissions of Diesel Engines. *Energies* **2016**, *9*, 28. [[CrossRef](#)]
20. Engin Özçelik, A.; Aydoğan, H.; Acaroğlu, M. Determining the performance, emission and combustion properties of camelina biodiesel blends. *Energy Convers. Manag.* **2015**, *96*, 47–57. [[CrossRef](#)]
21. Karthickeyan, V.; Balamurugan, P. Effect of thermal barrier coating with various blends of pumpkin seed oil methyl ester in DI diesel engine. *Heat Mass Transf.* **2017**, *53*, 3141–3154. [[CrossRef](#)]
22. Oerlikon Metco. *Material Product Data Sheet; Premium EBC-Grade Aluminum Silicate (Mullite) Powder [Brochure]*; Oerlikon Metco: Westbury, NY, USA, 2014.
23. Oerlikon Metco. *Material Product Data Sheet; 8% Yttria Stabilized Zirconia Agglomerated and HOSP™ Thermal Spray Powders [Brochure]*; Oerlikon Metco: Westbury, NY, USA, 2014.
24. MohamedMusthafa, M.; Sivapirakasam, S.P.; Udayakumar, M. A comparative evaluation of Al<sub>2</sub>O<sub>3</sub> coated low heat rejection diesel engine performance and emission characteristics using fuel as rice bran and pongamia methyl ester. *J. Renew. Sustain. Energy* **2010**, *2*, 053105. [[CrossRef](#)]
25. MohamedMusthafa, M.; Sivapirakasam, S.P.; Udayakumar, M. Comparative studies on fly ash coated low heat rejection diesel engine on performance and emission characteristics fueled by rice bran and pongamia methyl ester and their blend with diesel. *Energy* **2011**, *36*, 2343–2351. [[CrossRef](#)]
26. Senthil, R.; Sivakumar, E.; Silambarasan, R.; Pranesh, G. Performance and emission characteristics of using sea lemon biodiesel with thermal barrier coating in a direct-injection diesel engine. *Biofuels* **2016**, *8*, 235–241. [[CrossRef](#)]
27. Thiruselvam, K.; Ganesh, V. Performance and emission of diesel engine using thermal barrier coating and addition of cerium oxide nanoparticles to plam biodiesel. *J. Oil Palm Res.* **2019**, *31*, 138–145.
28. Das, D.; Sharma, K.R.; Majumdar, G. Review of Emission Characteristics of Low Heat Rejection Internal Combustion Engines. *Int. J. Environ. Eng. Manag.* **2013**, *4*, 309–314.
29. Behçet, R.; Oktay, H.; Çakmak, A.; Aydin, H. Comparison of exhaust emissions of biodiesel-diesel fuel blends produced from animal fats. *Renew. Sustain. Energy Rev.* **2015**, *46*, 157–165. [[CrossRef](#)]
30. Senthikumar, S.; Sivakumar, G.; Manoharan, S. Investigation of palm methyl ester biodiesel with additive on performance and emission characteristics of a diesel engine under 8 mode testing cycle. *Alex. Eng. J.* **2015**, *54*, 423–428. [[CrossRef](#)]
31. Karthickeyan, V.; Balamurugan, P.; Senthil, R. Environmental effects of thermal barrier coating with waste cooking palm oil methyl ester blends in a diesel engine. *Biofuels* **2017**, *10*, 207–220. [[CrossRef](#)]
32. Baukal, C.E., Jr. *The John Zink Hamworthy Combustion Handbook*, 2nd ed.; CRC Press: Tulsa, OK, USA, 2014; 1184p.
33. Öztürk, U.; Hazar, H.; Yilmaz, F. Comparative performance and emission characteristics of peanut seed oil methyl ester (PSME) on thermal isolated diesel engine. *Energy* **2019**, *167*, 260–268. [[CrossRef](#)]
34. Aydin, S.; Sayin, C. Impact of thermal barrier coating application on the combustion, performance and emissions of a diesel engine fuelled with waste cooking oil biodiesel-diesel blends. *Fuel* **2014**, *136*, 334–340. [[CrossRef](#)]
35. Aydin, S.; Sayin, C.; Altun, S.; Aydin, H. Effects of thermal barrier coating on the performance and combustion characteristics of a diesel engine fueled with biodiesel produced from waste frying cottonseed oil and ultra-low sulfur diesel. *Int. J. Green Energy* **2016**, *13*, 1102–1108. [[CrossRef](#)]
36. Tüccar, G.; Tosun, E.; Özgür, T.; Aydin, K. Diesel engine emissions and performance from blends of citrus sinesis biodiesel and diesel fuel. *Fuel* **2014**, *132*, 7–11. [[CrossRef](#)]

37. Hasimuglu, C.; Ciniviz, M.; Özsert, I.; Icingür, Y.; Parlak, A.; Salman, M.S. Performance characteristics of a low heat rejection diesel engine operating with biodiesel. *Renew. Energy* **2008**, *33*, 1709–1715. [[CrossRef](#)]
38. Mahalingam, A.; Munuswamy, D.; Devarajan, Y.; Radhakrishnan, S. Investigation on the emission reduction technique in acetone-biodiesel aspirated diesel engine. *J. Oil Palm Res.* **2018**, *30*, 345–349. [[CrossRef](#)]
39. Pandian, A.K.; Ramakrishnan, R.B.B.; Devarajan, Y. Emission analysis on the effect of nanoparticles on neat biodiesel in unmodified diesel engine. *Environ. Sci. Pollut. Res.* **2017**, *24*, 23273–23278. [[CrossRef](#)]
40. Devarajan, Y.; Munuswamy, D.B.; Mahalingam, A.; Arunkumar, T. Combustion, performance and emission study of a research diesel engine fueled with palm oil biodiesel and its additive. *Energy Fuel* **2018**, *32*, 8447–8452. [[CrossRef](#)]
41. Devarajan, Y.; Munuswamy, D.B.; Mahalingam, A.; Nagappan, B. Performance, combustion, and emission analysis of neat palm oil biodiesel and higher alcohol blends in a diesel engine. *Energy Fuels* **2017**, *31*, 13796–13801. [[CrossRef](#)]